Investigation of Thermocapillary Convection of High Prandtl Number Fluid Under Microgravity

Ruquan Liang, Guangdong Duan

Key Laboratory of National Education Ministry for Electromagnetic Processes of Materials, Northeastern University, No.3-11, Wenhua Road, Shenyang 110819, China

Keywords: Liquid Bridge, Thermocapillary Convection, Velocity, Temperature

Abstract

Thermocapillary convection in a liquid bridge, which is suspended between two coaxial disks under zero gravity, has been investigated numerically. The Navier-Stokes equations coupled with the energy conservation equation are solved on a staggered grid, and the level set approach is used to capture the free surface deformation of the liquid bridge. The velocity and temperature distributions inside the liquid bridge are analyzed. It is shown from this work that as the development of the thermocapillary convection, the center of the vortex inside the liquid bridge moves down and reaches an equilibrium position gradually. The temperature gradients in the regions near the upper center axis and the bottom cold corner are higher than those in the other regions.

1. Introduction

Thermocapillary flow is often encountered in the production of single crystals using the floating-zone method, and the oscillatory thermocapillary convection is responsible for the periodic variations in striations in the production process. The oscillatory thermocapillary convection becomes significant and causes detrimental striations in the chemical composition of the finished crystal. Schwabe and Scharmann[1] and Chun and Wuest[2] observed, for the first time, the three-dimensional time-dependent state in thermocapillary convection in their experiments. Since the first observation, many studies have been done on the half-zone model where a liquid drop is held between two coaxial rods remained at different temperatures to impose an axial temperature gradient on the free surface, and the liquid drop is held by surface tension force between two rods. The studies found in the literature mainly concerned with the following aspects,

1. The transition and the successive mode structures of the flow field[3-6],
2. The flow structures at a region close to the critical point of the transition,
3. The information regarding the flow fields far beyond the critical point[7].

In the high Pr range (Pr>10), although many experimental data can be found in literature, no accurate stability analyses nor numerical simulations of the oscillation phenomenon are currently available. One important aspect is that the dynamic free surface deformation was not considered, although it may play an important role in the oscillation mechanism. In the present paper, the temperature and velocity fields in the liquid bridge under zero gravity are investigated numerically considering the free surface deformation and the ambient air by using the level set method. The present study aims at understanding the time dependent thermal fluid phenomena with dynamic free surface deformation in the half-zone liquid bridge by a direct nonlinear numerical simulation.

2. Governing Equations

The half-zone model consists of an initially cylindrical liquid bridge suspended between the hot and cold circular disks as shown in Figure 1. The ambient air is included in the computational region. The diameter of the top and bottom disks (D) is 5.0 mm, and the aspect ratio of the liquid bridge (H/D) is 0.7, where H is the height of the liquid bridge. The temperature difference between two disks is defined as ΔT. The general governing equations of the problem

for Newtonian incompressible flow conditions under zero gravity are given by the following non-dimensional Navier-Stokes, the continuity and the energy conservation equations[8].

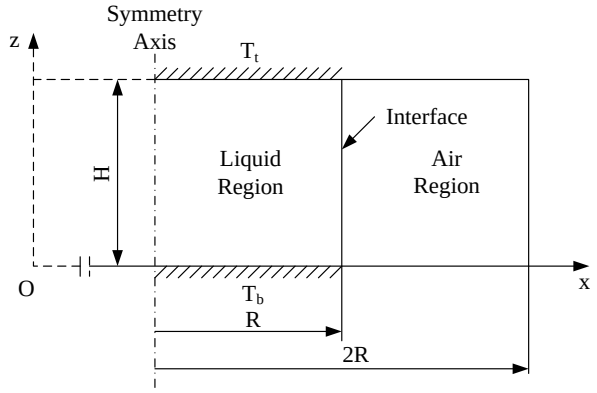

Figure 1. Schematic of a thermocapillary convection model

$$\mathbf{u}_t + (\mathbf{u}\cdot\nabla)\mathbf{u} = \frac{1}{\rho}\left(-\nabla p + \frac{1}{\mathrm{Re}}\nabla\cdot(2\mu\mathbf{D}) + \left(\frac{1}{\mathrm{We}} - \frac{\mathrm{Ca}}{\mathrm{We}}\Theta\right)\kappa\delta(d)\mathbf{n}\right) \tag{1}$$

$$\nabla\cdot\mathbf{u} = 0 \tag{2}$$

$$\frac{\partial\Theta}{\partial t} + \nabla\cdot(\mathbf{u}\Theta) = \frac{1}{\mathrm{Re}\,\mathrm{Pr}}\nabla^2\Theta \tag{3}$$

where $\mathbf{u} = (u, v)$ is the fluid velocity, $\rho = \rho(\mathbf{x}, t)$ is the fluid density, $\mu = \mu(\mathbf{x}, t)$ is the fluid viscosity, $\mathbf{D}$ is the viscous stress tensor, κ is the curvature of the interface, d is the normal distance to the interface, δ is the Dirac delta function, $\mathbf{n}$ is the unit normal vector at the interface, t is the time, p is the pressure. The key parameters are $\mathrm{Re} = \rho_l U_\infty D/\mu_l$, Reynolds number, where D is the initial diameter of the liquid bridge and U_∞ is the characteristic velocity defined as $U_\infty = \sigma_T \Delta T / \mu_l$ in microgravity conditions, where σ_T is the temperature dependency of surface tension, $\Delta T = T_t - T_b$ is the temperature difference between the top and bottom disks; $\mathrm{We} = U_\infty^2 D\rho_l/\sigma$, Weber number; $\mathrm{Pr} = \mu_l/\rho_l a$, Prandtl number, where a is the thermal diffusivity; $\mathrm{Ca} = \mu_l U_\infty/\sigma$, Capillary number; $Ma = \mathrm{Re}\,\mathrm{Pr}$, Marangoni number. We denote σ as the surface tension, $\sigma = \sigma_c - \sigma_T(T - T_b)$, where σ_c is a reference value of surface tension, and Θ as the excess temperature, $\Theta = (T - T_b)/\Delta T$. Here ρ_l and μ_l are the dimensional liquid density and viscosity, respectively. ρ_g and μ_g are the dimensional density and viscosity of ambient air, respectively.

3. Level Set Function and Its Formulation

The level set method was originally introduced by Osher and Sethian (1988)[9] to numerically predict the moving interface $\Gamma(t)$ between two fluids. Instead of explicitly tracking the

interface, the level set method implicitly captures the interface by introducing a smooth signed distance from the interface in the entire computational domain. The level set function $\phi(\mathbf{x},t)$ is taken to be positive outside the liquid bridge, zero at the interface and negative inside the liquid bridge. The interface motion is predicted by solving the following convection equation for the level set function of $\phi(\mathbf{x},t)$ given by[10],

$$\phi_t + \mathbf{u}\cdot\nabla\phi = 0 \tag{4}$$

$$\mathbf{u}\cdot\nabla\phi = (u\phi)_x + (v\phi)_y \tag{5}$$

$$(u\phi)_x + (v\phi)_y = u_{i+1/2,j}(\phi_{i+1,j} - \phi_{i,j})/(2h) + \phi_{i+1/2,j}(u_{i+1,j} - u_{i,j})/(2h)$$
$$+ v_{i,j+1/2}(\phi_{i,j+1} - \phi_{i,j-1})/(2h) + \phi_{i,j+1/2}(v_{i,j+1} - v_{i,j-1})/(2h)$$

For smooth data, we have $(\phi_{i+1/2,j} + \phi_{i-1/2,j}) \approx (\phi_{i,j+1/2} + \phi_{i,j-1/2})$. In addition, we have $(u_{i+1/2,j} - u_{i-1/2,j}) \approx (v_{i,j+1/2} - v_{i,j-1/2})$ because $\mathbf{u}$ is numerically divergence free. Thus,

$$(u\phi)_x + (v\phi)_y \approx (u_{i+1/2,j} + u_{i-1/2,j})(\phi_{i+1/2,j} - \phi_{i-1/2,j})/(2h)$$
$$+ (v_{i,j+1/2} + v_{i,j-1/2})(\phi_{i,j+1/2} - \phi_{i,j-1/2})/(2h)$$

In addition, the model of Continuum Surface Force (CSF) is employed to treat the surface tension force on the interface, which interprets the surface tension force as a continuous body force across the interface rather than as boundary conditions in normal and tangential directions to the interface. By using the level set function, body force due to surface tension can be expressed as,

$$\frac{1}{\mathrm{We}}\kappa\delta(d)\mathbf{n} = \frac{1}{\mathrm{We}}\kappa(\phi)\delta(\phi)\nabla\phi$$

The curvature of the interface is evaluated from

$$\kappa(\phi) = -\nabla\cdot(\mathbf{n})$$

$$\nabla\cdot\mathbf{n} = \nabla\cdot\left(\frac{\nabla\phi}{|\nabla\phi|}\right)$$

The Dirac delta function is defined as

$$\delta_\alpha(\phi) \equiv \begin{cases} \frac{1}{2}\left(1+\cos(\pi\phi/\alpha)\right)/\alpha, & if\ |\phi| < \alpha \\ 0, & otherwise \end{cases}$$

4. Boundary and Initial Conditions

The flow in the liquid bridge is assumed to be axis-symmetric initially, and the hot and cold disks are maintained at constant temperature T_t and T_b, respectively.

$$\Theta = 0 \quad (z = 0)$$

$$\Theta = 1.0 \quad (z = 1.0)$$

The adiabatic condition is adopted on the all other boundary walls expect for the hot and cold disks. The initially stationary liquid bridge and the ambient air are considered with the initial condition

$$\mathbf{u}(t = 0) = 0$$

The non-slip condition is used for all walls of the computational domain

$$\mathbf{u} = 0$$

The present strategy is further summarized below. The mass conserving level set methods is applied to analyze the free surface motion of the liquid bridge. The Navier-Stokes equations in primitive variable formulations and energy conservation equation are solved on a staggered grid by the method of lines. The advection terms are discretized by the quadratic upstream interpolation for convective kinematics (QUICK) method and the other terms by the central finite difference method except for the body force, and a second-order Adams-Bashforth method is used as the time integration scheme. The higher essentially non-oscillatory (ENO) scheme is also adopted to solve the convection term of the level-set function. The Poisson equations are solved by means of the Successive Over Relaxation (SOR) approach. The Continuum Surface Force (CSF) model is employed to treat the surface tension force at the interface.

5. Code Validation

In present study, the numerical model and code have been carefully tested again by comparing the isotherms and velocity vectors in the liquid bridge of 2cSt silicone oil obtained from the present study with those reported by Kawamura et al.[11]. In the comparison, the initial liquid bridge and the ambient air are denoted to be stationary and axis-symmetric. The radii and height of the liquid bridge are $R = 5\,\mathrm{mm}$, $H = 5\,\mathrm{mm}$, respectively. The temperature difference between the top and bottom disks is $\Delta T = 30°C$. The Marangoni number is $Ma = 4 \times 10^4$, and the Prandtl number is $\mathrm{Pr} = 28.0$. The temperature contour and velocity vectors obtained from the present work under zero gravity is shown in Figure 2, and the agreement between the present results and those from Kawamura et al. can be qualified as quite acceptable (see Fig. 5(b) of Kawamura et al. (2007)).

6. Results and Discussion

The mechanism of thermocapillary convection in a liquid bridge of high Prandtl number under zero gravity is investigated. The key parameters used are as follows: $\mathrm{Pr} = 50$, $Ma = 5000$, $We = 15$, $T_t = 328K$, $T_b = 298K$. Diameter of the top and bottom disks is $D = 5.0mm$, and the aspect ratio (H / D) is 0.7. In this section, we study the flow structure inside the liquid bridge under the present computational conditions.

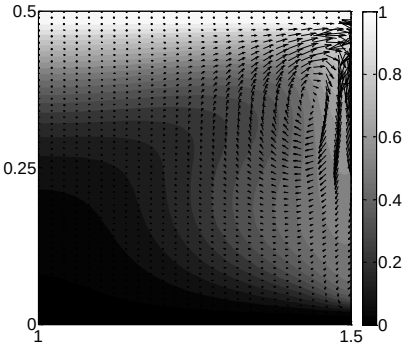

Figure 2. Temperature contour and velocity vectors (2cSt silicone oil, $Ma = 4 \times 10^4$, $\Pr = 28.0$)

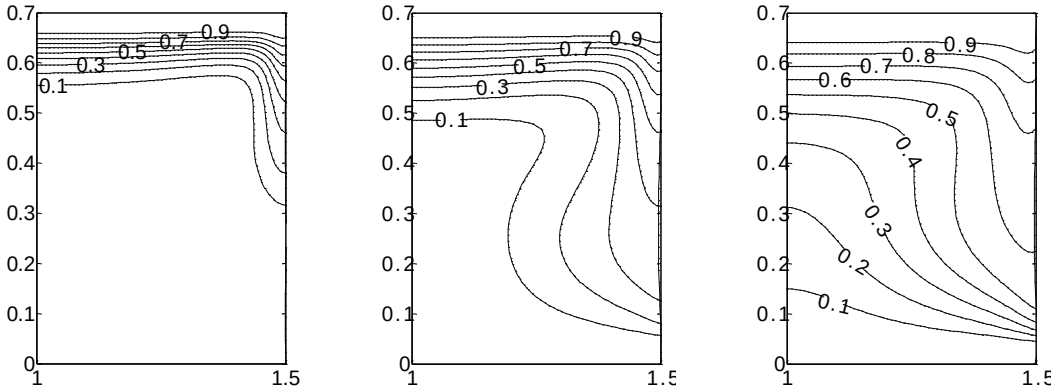

t=2.0 *t*=15.0 *t*=200.0

Figure 3 Time evolution of isothermals ($\Pr = 50$, $Ma = 5000$, $We = 15$, $T_t = 328K$, $T_b = 298K$, $D = 5.0mm$, $H / D = 0.7$)

Figure 3 illustrates time evolution of isothermals inside the liquid bridge, where only half of the liquid bridge is plotted. Since the temperature of the top disk is higher than that of the bottom disk, the heat flux moves from the top disk toward the bottom disk, and the flow is driven in the hot corner. On the other hand, the surface flow is developed due to the temperature gradient on the free surface, which results in a return flow inside the liquid bridge. The return flow generates a radial convection, which tends to make the bulk fluid temperature distribution rather uniform near the free surface. It can be found from Figure 3 that the temperature gradients in the regions near the upper center axis and the bottom cold corner are higher than those in the other regions.

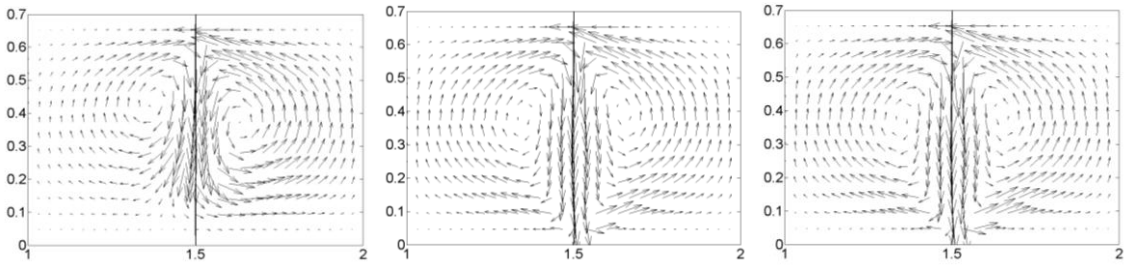

t=2.0 *t*=50 *t*=100.0

Figure 4 Time evolution of velocity vectors ($\Pr = 50$, $Ma = 5000$, $We = 15$, $T_t = 328K$, $T_b = 298K$, $D = 5.0mm$, $H / D = 0.7$)

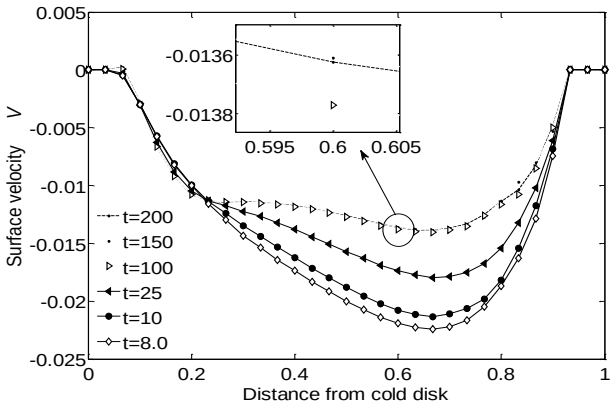

Figure 5 Time evolution of surface velocity in axial direction ($\mathrm{Pr} = 50$, $Ma = 5000$, $We = 15$, $T_t = 328K$, $T_b = 298K$, $D = 5.0mm$, $H / D = 0.7$)

The velocity vectors in the liquid bridge and ambient air at *t*=2.0, *t*=50.0, and *t*=100.0 are presented in Figure 4. Note that only half of the computational domain is plotted in Figure 4 due to the symmetric property. The free surface remains straight shape due to the zero gravity. Two vortexes are generated due to the thermocapillary convection inside the liquid bridge and ambient air, respectively, and the vortex center inside the liquid bridge locates near the hot corner initially (*t*=2.0) as shown in Figure 4. As the development of the thermocapillary convection, the vortex center inside the liquid bridge moves down and reaches an equilibrium position gradually (*t*=50.0, *t*=100.0). The larger velocity vectors can be found mainly around the free surface because the flow is driven by the surface flow generated near the free surface. Figure 5 shows the surface velocities in axial direction. It can be seen that the values of the surface velocities in axial direction are all negative, showing that the direction of the surface flow is from the top disk toward the bottom disk. The surface velocities in axial direction at the top disk and the bottom disk are zero due to the no-slip conditions in there. As the time proceeds (*t*=8.0, *t*=10.0, *t*=25.0, *t*=100.0), the levels of the surface velocities in axial direction rise, showing the enhancement of the surface flow gradually. After that, the profiles at *t*=100.0, *t*=150.0, and *t*=200.0 are very close, showing the surface flow approaches the equilibrium state after *t*=100.0. The maximum of the surface velocities in axial direction can be obtained on the surface position of about z=0.65 at every time, where z is the non-dimensional distance from the cold disk.

7. Conclusions

Thermocapillary convection in a liquid bridge of $\mathrm{Pr} = 50$ under zero gravity has been investigated numerically. From this work, the following conclusions can be drawn.

1. The temperature gradients in the regions near the upper center axis and the bottom cold corner are higher than those in the other regions.

2. As the development of the thermocapillary convection, the vortex center inside the liquid bridge moves down and reaches an equilibrium position gradually.

3. As the time proceeds, the levels of the surface velocities in axial direction rise, showing the enhancement of the surface flow gradually. After that the surface flow approaches the equilibrium state. The maximum of the surface velocities in axial direction can be obtained on

the surface position of about z=0.65 at every time, where z is the non-dimensional distance from the cold disk.

Acknowledgement

The present work is supported financially by the National Natural Science Foundation of China under the grant of 11072057 and the Natural Science Foundation of Liaoning Province under the grant of 20092002.

References

1. D. Schwabe, A. Scharmann, "Steady and oscillatory Marangoni convection in floating zones under microgravity," *J. Cryst. Growth*, 6(1979), 125.

2. C. H. Chun, W. Wuest, "Experiments on the transition from the steady to the oscillatory marangoni-convection of a floating zone under reduced gravity effect," *Acta Astronaut.*, 6(9)(1979), 1073-1082.

3. F. Preisser, D. Schwabe, and A. Scharmann, "Steady and oscillatory thermocapillary convection in liquid columns with free cylindrical surface," *J. Fluid. Mech.*, 126(1983), 545-567.

4. Y. Kamotani, S. Ostrach, and M. Vargas, "Oscillatory thermocapillary convection in a simulated floating-zone configuration," *J. Cryst. Growth*, 66(1984), 83-90.

5. R. Velten, D. Schwabe, and A. Scharmann, "The periodic instability of thermocapillary convection in cylindrical liquid bridges," *Phys. Fluids*, 3(A) (1991), 267-280.

6. J. Masud, Y. Kamotani, and S. Ostrach, "Oscillatory thermocapillary flow in cylindrical columns of high Prandtl number fluids," *J. Thermophys. Heat Transfer*, 11(1997), 105.

7. S. Frank , D. Schwabe, "Temporal and spatial elements of thermocapillary convection in floating zones," *Exp. Fluids*, 23(1997), 234.

8. R. Q. Liang , Z. Chen, "Dynamics for droplets in normal gravity and microgravity," *Microgravity Sci. Technol.*, 21(2009), 247-254.

9. S. Osher, J. Sethian, "Fronts propagating with curvature-dependent speed: Algorithms based on hamilton-jacobi formulations," *J. Comput. Phys.*, 79(1) (1988), 12-49.

10. M. Sussman, P. Smereka, and S. Osher, "A level set approach for computing solutions to incompressible two-phase flow," *J. Comput. Phys.*, 114 (1994), 146-159.

11. H. Kawamura, E. Tagaya, and Y. Hoshino, "A consideration on the relation between the oscillatory thermocapillary flow in a liquid bridge and the hydrothermal wave in a thin liquid layer," *Int. J. Heat Mass Tran.*, 50(2007), 1263-1268.